ГЛАСНИК Српског географског друштва 100(2) 1 – 23
BULLETIN OF THE SERBIAN GEOGRAPHICAL SOCIETY 2020

Original scientific paper
UDC 551.4(267)
https://doi.org/10.2298/GSGD2002001L

Received: October 07, 2020
Corrected: November 27, 2020
Accepted: December 09, 2020

Polina Lemenkova[1*]

[*] *Schmidt Institute of Physics of the Earth, Russian Academy of Sciences, Department of Natural Disasters, Anthropogenic Hazards and Seismicity of the Earth, Laboratory of Regional Geophysics and Natural Disasters, Moscow, Russian Federation*

JAVA AND SUMATRA SEGMENTS OF THE SUNDA TRENCH: GEOMORPHOLOGY AND GEOPHYSICAL SETTINGS ANALYSED AND VISUALIZED BY GMT

Abstract: The paper discusses the geomorphology of the Sunda Trench, an oceanic trench located in the eastern Indian Ocean along the Sumatra and Java Islands of the Indonesian archipelago. It analysis difference in depths and variation in slope steepness between the two segments of the trench: southern Java transect (108.8°E 10.10°S - 113.0°E 10.75°S) and northern Sumatra transect (97.5°E 1.1°S - 101.0°E 5.5°S). The maps and geomorphological modelling were plotted using Generic Mapping Tools (GMT). The data include high-resolution grids on topography, geology, geodesy and geophysics: GEBCO, EGM2008 EGM-2008, GlobSed. The results include modelled segments, slope gradients, and cross-section profiles. The geological processes take place in the Indian Ocean at different stages of its evolution and influence the nature of the submarine geomorphology and geomorphology of the trench that differs in two segments. Java segment has a bell-shaped data distribution in contrast to the Sumatra with bimodal pattern. Java segment has the most repetitive depths at -2,500 to -5,200 m. Sumatra transect has two peaks: 1) a classic bell-shaped peak (-4,500 m to -5,500 m); 2) shelf area (0 to -1,750 m). The data at middle depths (-1,750 to -4,500 m) have less than 300 samples. The most frequent bathymetry for the Sumatra segment corresponds to the -4,750 m to -5,000 m. Comparing to the Sumatra segment, the Java segment is deeper. For depths > -6,000 m, there are only 138 samples for Sumatra while 547 samples for Java. Furthermore, Java segment has a more symmetrical geometric shape while Sumatra segment is asymmetric, one-sided. The Sumatra segment has a steepness of 57.86° on its eastern side (facing Sumatra Island) and a contrasting 14.58° on the western part. The Java segment has a steepness of 64.34° on its northern side (facing Java Island) and 24.95° on the southern part (facing the Indian Ocean). The paper contributes to the studies of the submarine geomorphology in Indonesia.

Key words: Submarine Geomorphology, GMT, Sunda Trench, Indian Ocean, geology, cartography, mapping

[1] pauline.lemenkova@gmail.com (corresponding author)

Introduction

The study is focused on the Sunda Trench (also earlier called Java Trench), the deepest oceanic depression of the Indian Ocean, stretching 4–5 km parallel to the Sunda Island Arc, along its foot (Becker et al., 2009). Geographically, it stretches in the roughly northwest-southeast direction starting from the Andaman Islands, along the Indonesian archipelago, Sumatra, Java and the Lesser Sunda Islands until the Island of Timor (Plank & Langmuir, 1994; Harris et al., 2014; Dewi et al., 2019). Its seafloor bottom has irregular characters being wider (up to 50 km) in its northern part and gradually becoming narrow in the south (up to 10 km). The region of Sunda Volcanic Arc includes the islands of Sumatra and Java, the Sunda Strait between them, and the Lesser Sunda Islands stretching between 5 and 10° S (Fig. 1).

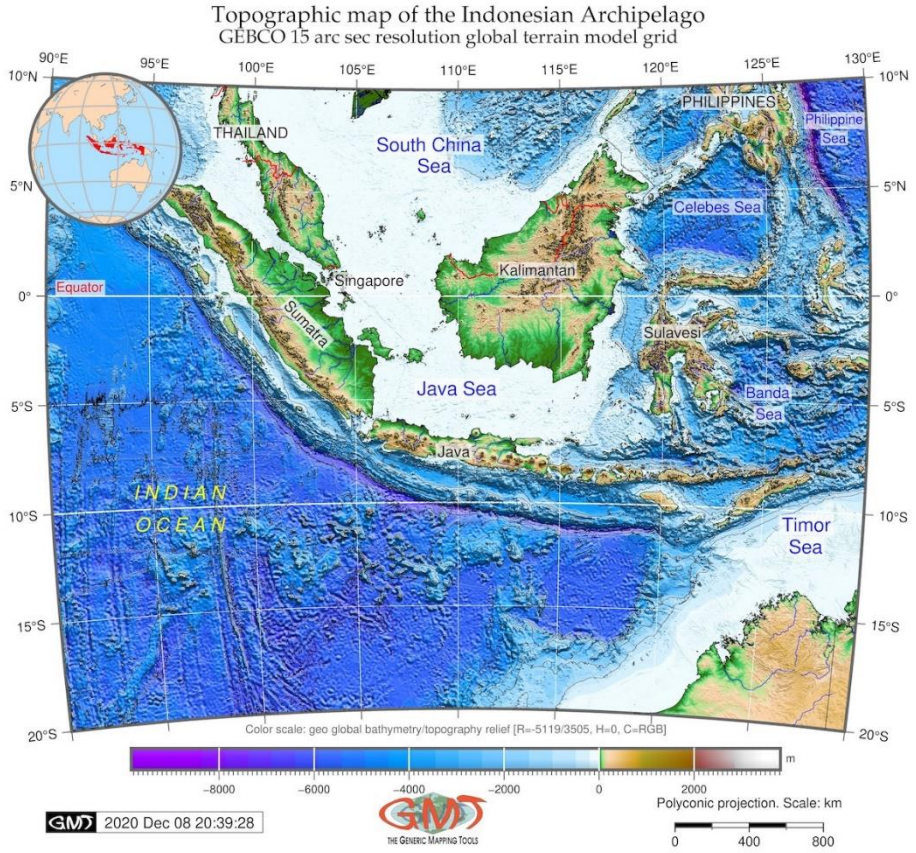

Fig. 1. Topographic map of the West Indonesia region Basin (Source: Author)

The depths of the seafloor of the Sunda Trench increase from the northwest (-3,000 m) to the southeast (-6,000 m), and reach the maximum depth with 7,209 m. Further to the east, the short Timor Trough (3,310 m) continues the Sunda Trench marking the boundary between the Indo-Australian Plate and the Timor Plate (Haryanto et al., 2020).

It is separated by a threshold from the Seram Trough at Kai Islands Arch (-3,680 m). The Indonesian archipelago has a complex geological structure reviewed in many relevant publications (Charlton, 2000; Elburg et al., 2005; Chlieh et al., 2008; Ely & Sandiford, 2010; Verstappen, 2014; Tabei et al., 2015; Winarto et al., 2019).

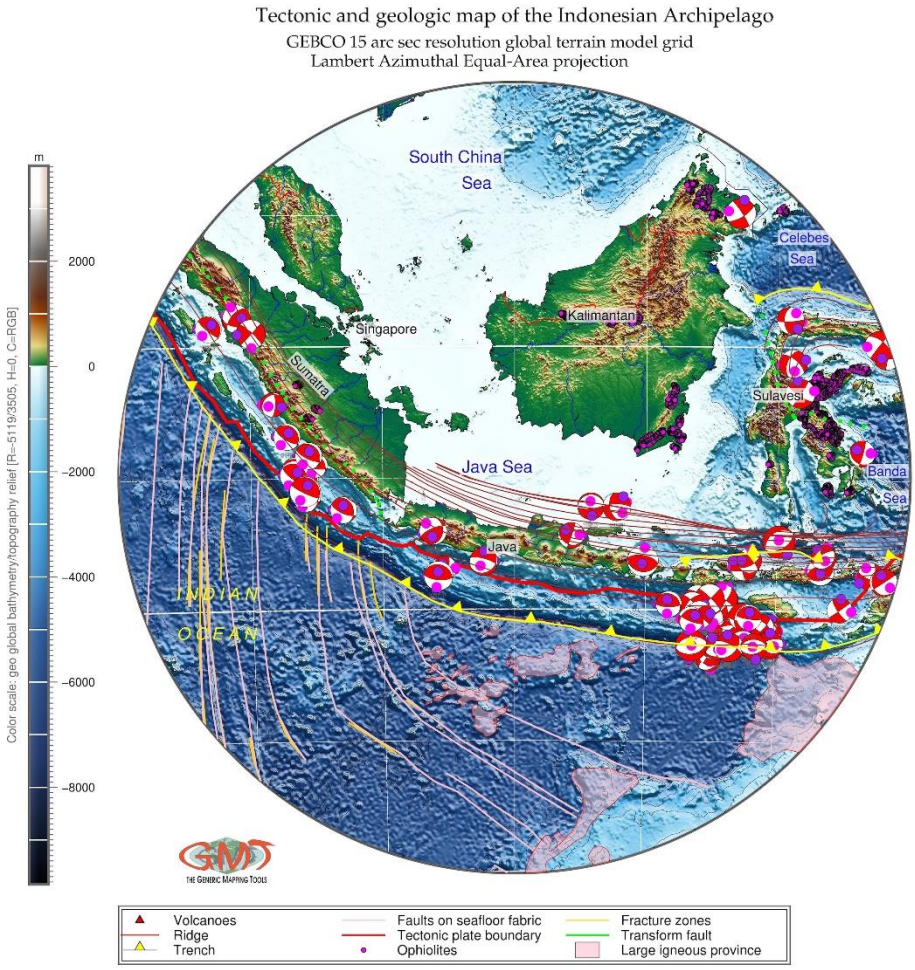

Fig. 2. Geologic map of the West Indonesia Basin (Source: Author)

The northwestern part of the arc is bordered by the Andaman Sea which has a wide shelf in the east (with depths less than 100 m) and an oval basin in the west. The seafloor bottom of the basin is dissected into a number of local troughs by a series of the submeridional submarine uphills with depths exceeding -4,000 m in its western part. The complexity of the tectonic setting in the region is illustrated by the presence of three major plates: Eurasian, the Indian, and the Australian with the Australian Plate diving under the Sunda Plate forming a subduction zone (Sieh & Natawidjaja, 2000). The Indonesian segment of the Eurasian plate has been divided into three minor and microplates that include: the Sunda Plate, the Banda Sea Plate, the Molucca Plate and the Timor Plate. Details on the tectonic evolution on the region are described (Megawati &

Pan, 2010; Ashadi & Kaka, 2019; Harris et al., 2020). The movement of the Australian Plate northwest relative to the Wadati–Benioff Zone resulted in the formation of the Sunda trench-arc system. Local basin depressions of the Indian Ocean formed in the eastern part of the Sunda Island Arc and east of New Guinea where the structures were oriented across the main tectonic plate movement and experienced local rotations. As a consequence, such tectonic processes governing the evolution of the Indian Ocean give rise to different geomorphic features as long as they pass through the different periods of geologic evolution.

The region of Sunda land was formed during the late Paleozoic (Late Permian) and early Mesozoic (Triassic) periods as a result of the amalgamation of continental and arc fragments in Indochina, Thailand, Malaysia and Sumatra. Based on the wide distribution of the Mesozoic marine deposits found on the Sunda Island Arc, there was a deep-sea basin that existed between Australia and Indochina during Jurassic period of Mesozoic. This basin was connected with the Pacific Ocean in the east, and with the Tethys Ocean in the west. The presence of this basin on the territory of the modern Sunda Island Arc points to the disintegration of the Gondwana, which occurred at the next period of its geological development. As a result of the seafloor expansion, the oceanic plate subducted under the continental Indo-Australian and Eurasian plates on the eastern border of Tethys during Cretaceous. During Paleogene, the rift zone of Tethys Ocean reduced due to the northward movement of Australia. As a consequence, its seafloor also moved northward, being absorbed in the Wadati-Benioff Zone under the system of Sunda Island Arc. The oceanic passage from the Indian Ocean to the Pacific Ocean northward off Australia still existed at the end of the Eocene, although much narrower. The Sunda trench-arc system was formed as a result of the complex tectonic movements in course of the geological history of the east Indian Ocean that are reviewed in relevant published literature on geology and tectonic evolution of the Indonesian archipelago region (Audley-Charles et al., 1988; Nishimura & Suparka, 1990; Gasparon et al., 1994; Hughes et al., 1996; Honthaas et al., 1998; Kreemer et al., 2000; Hinschberger et al., 2001; Audley-Charles, 2004; Das, 2004).

Geological processes and phenomena that take place in bathymetric basins at different stages of ocean evolution influence the nature of geomorphology and the geometric shape of the deep-sea trenches. The plate subduction and uplifting driving mechanisms across the Indonesian region have acted remarkably during Cenozoic (Patria & Aulia, 2020). The most important, among the many geologic processes that generate and shape the geomorphology of the slopes of the Sunda Trench is the subduction of the tectonic plate which includes bending of the oceanic lithosphere. Other geological factors affecting the formation of the oceanic trenches include volcanism and sedimentation (Kawamura et al., 2017; Lemenkova, 2018, 2019a; Kawamura et al., 2020). As a result of the variety of factors, the submarine geomorphology of the Indonesian region was formed. Its geomorphological features include rift valleys, spreading ridges, local minor troughs, and a Sunda Trench. The subduction of the plate starts many kilometers off the trench axis, being caused by the buoyance of the tectonic slab and the elastic nature of the lithosphere. The beginning of the plate bending is noted by the outer rise, a bathymetric high on the seaward side of the trench (facing the Indian Ocean, opposite from Indonesia).

The crystalline basement surface of Cenozoic structures on the Sunda Island Arc almost coincides with the modern bathymetry forming two ridges: the main ridge and outer ridge, separated by a longitudinal trough with depths of up to 2-4 km. The outer ridge has a steep slope to the Sunda Trench where depths reach up to -6,000 m. The sedimentary cover on the steep slopes of the Sunda Island Arc is generally thin increasing only in local depressions. The thickness of the Cenozoic deposits exceeds 1 km on the seafloor of the Sunda Trench. The lower seafloor layer on the island arcs and submarine ridges, hills, and elevations at the bottom of the basin is mainly presented by the granite and metamorphic rocks of the continental crust, especially for the large islands, formed as folded mountain structures. The structure of the rocks of the Sunda trench-arc system points at Paleozoic schists and gneisses, other metamorphic rocks, granite intrusions, and occasional turbidite accumulation in the seafloor of the trench (Pickering et al., 2020).

The geomorphology framework of the Sunda Trench is largely controlled by the subduction of the Australian plate underneath the Sunda microplate. The geological processes take place in the basin of the Indian Ocean at different stages of its evolution and influence the nature of the submarine geomorphology and geometric shape of the trench. Sunda Trench is a seismically active part of the Pacific Ring of Fire. A large number of catastrophic earthquakes are recorded around the trench. Sunda Trench is seismically active, being a part of the Pacific Ring of Fire. The seismic belt around it connects the Alpide orogenic system and the circum-Pacific seismic belt. A large number of catastrophic earthquakes are recorded in this region (McCloskey et al., 2010; Nalbant et al., 2013; Gunawan et al., 2017; Salman et al., 2020). The hypocentres of the earthquake surfaces are located under the Sunda Trench and Sunda Island Arc (Nalbant et al., 2005) which ultimately affect the geomorphological shape of the seafloor (Nurwihastuti et al., 2014). The hypocenters of intermediate earthquakes (focal depth at 60–300 km) and deep-focus earthquakes (focal depth > 300 km) form a focal zone with varying inclination: depth of ca. 300 km is 35°, and depth > 300 km is up to 60°, which indicates at the fracture of the subducted oceanic plate. The morphology and depth of the subducted plate are defined by the earthquake hypocenters that vary along the plate boundaries. Thus, the crust under the Sunda Island Arc is up to 25 km thick. It is composed of a thin layer with seismic wave velocities of 3.9-4.7 km/s and much more thick main layers with wave velocities of 5.1-5.7 and 6.6-7.2 km/s typical for solid crustal rocks. Under the seafloor bottom of the Sunda Trench, the crustal thickness decreases to 14 km with layers having seismic velocities of 4.1 and 7.2 km/s. More detailed studies on the seismicity and earthquakes in the Indonesian region and Sunda Trench area exist in published literature (Natawidjaja & Triyoso, 2007; Harris, 2011; Maemunah et al., 2015; Lemenkova, 2020b).

Material and Methods

As described above, the Java-Sumatra region is notable for the complexity of the tectonic processes in the active convergent tectonic plate margin marked by the subduction of the Indo-Australian Plate under the Eurasian Plate. Necessarily, numerical methods of data processing are required to model the specifics and reconstruct the past Sumatra and Java tectonic movements, as presented in previous studies, for instance, geodetic and paleogeodetic measurements (Chlieh et al., 2008). Other approaches include, for example, used tsunami modelling (Saito & Kubota, 2020), method of the r40Ar/39Ar

geochronology of volcanic and intrusive rocks was applied for analysis of the geological prospects in the West Java (Titisari et al., 2017). Development of the mapping methods is presented in marine cartography and visualization, as well as automatization approaches in the GIS techniques (Schenke & Lemenkova, 2008; Lemenkova, 2019e, 2020e, 2020g).

The method used to perform cartographic visualization, modelling and mapping is based on the Generic Mapping Tools (GMT). The GMT is developed in 1991 and works as a scripting toolset of modules from a shell console. Since then, it has been used in geophysical and topographic mapping and being continuously developed since then (Wessel et al., 2013). The GMT has embedded vector shorelines and contours of major geographical objects (rivers, lakes, borderlands) for the World as a basis map used in this research (Wessel & Smith, 1996). For example, a group of modules (such as gmtset, gmtdefaults, grdcut, makecpt, grdimage, psscale, grdcontour, psbasemap, gmtlogo, psconvert and many others) was taken together to perform topographic mapping by a group of sub-tasks: subset raster grid from a raw file, to define projection, visualize, add cartographic elements, and convert the layout output to a graphical format. All this is done sequentially, in a GMT shell script consisting of a sequential line of code, similar to the principle of programming.

The examples of the existing GMT scripting are provided in the existing papers on using GMT for geomorphological mapping with a detailed description of the GMT modules (e.g., Lemenkova, 2020a, 2020c, 2020h). A GMT approach is facilitated by a process division into sub-tasks and one or more modules "responsible" for executing these tasks that visualize certain cartographic elements (e.g., add annotations, coasts, visualize raster image from a grid, add a color legend, add information about projection, defile grid on the cartographic layout, etc.) and solutions by sketching them out on maps. To a certain extent, this principle can be compared to the structure of layers in a standard GIS menu, e.g., in the ArcGIS (Suetova et al., 2005; Gohl et al., 2006a, 2006b; Kuhn et al., 2006; Lemenkova, 2011; Lemenkova et al., 2012; Klaučo et al., 2014, 2017). The result of a GMT data processing consists in the print-quality series of maps, geomorphological models, and descriptive statistical analysis.

The importance of the precision and accuracy of the raw topographic and geophysical data for mapping has been discussed previously (Weatherall et al., 2015). Therefore, high-resolution data were selected as the materials for this research: the topography based on the GEBCO 15-arc second resolution grid (GEBCO Compilation Group, 2020) which is using SRTM basemap (Tozer et al., 2019), geoid based on the 2.5 minute Earth Gravitation Model of 2008 (EGM2008) raster grid (Pavlis et al., 2012), vector layers from the repository of Scripps Institution of Oceanography (SIO), U.S., marine free-air gravity grid (Sandwell et al., 2014), data on tectonic plate boundaries and movements, geological data on earthquakes from the global CMT project (Ekström et al., 2012), tectonic plates boundaries (Bird, 2003). Sediment thickness data were taken from the GlobSed global 5-arc-minute total sediment thickness dataset (Straume et al., 2019). The information on the data layers, extend on the topographic range (depths) and projections were retrieved using (Geospatial Data Abstraction Library) GDAL (GDAL/OGR contributors, 2020). The cross-section profiling was done using "grdtrack" module of GMT by automated digitizing of the profile transects crossing the trench in a perpendicular direction in two selected segments.

Results

As a result of complex geological settings and tectonic evolution, the geomorphology of the Sunda Trench region is rather complex and varying. The outer slope of the Sunda Island Arc has a typical convex profile and stepped structure. The ridge of the Sunda Island Arc is formed here by massive submarine narrow elevations with stepped slopes. In general, the Sunda Island Arc is formed as a double arc stretching in a southeast direction to the New Guinea. The islands of Sumatra, Java, and Lesser Sunda Islands (Sumbawa and Flores and others) are located on its inner ridge. The outer ridge is much narrower with the small islands of Nias Island, located off the western coast of Sumatra, and a chain of Mentawai Islands Regency rising on its western part. The islands of Sumba, Timor, a group of Tanimbar Islands, and Seram are located in the east of the Sunda Island Arc (IHO-IOC, 2012). The submarine ridges are separated by a longitudinal trough consisting of the successively located narrow depressions, with depths gradually increasing from the NW (-1,000 to -1,500 m) to the SE (-3,700 to -4,000 m). More descriptions of the geomorphology of the Sunda region are given by Poetra et al. (2020).

The seafloor bottom of the trench varies being different in the segments off Sumatra and Java. Southeast of Java it is presented by a series of local depressions separated by uphills. Comparing to other oceanic trenches, such as Tonga, Kermadec, Yap and Palau, Kuril-Kamchatka, Ryukyu and modelling seafloor (Lemenkova, 2019b, 2020d, 2020i), the slopes of the Sunda Trench are generally steeper and asymmetric. The asymmetry of the slopes in different geometry of its oceanic and landward sides: comparing to the oceanic slope, the landward slope is higher and steeper, more dissected by canyons and complicated by steps and ledges. In the Sumatra and northern Java segment, the seafloor bottom is up to 35 km wide, leveled by a layer of terrigenous sediments with a large admixture of volcanic material, the thickness of which reaches 3 km in the north. The Sunda outer ridge stretches several hundred meters high, divided into two parts by a saddle along the Sunda Trench. Some block structures and separate seamounts rise with a height of 2,000-3,000 m rise on its convex surface.

The main topographic map of the region is based on the GEBCO grid (Fig. 1). The geologic data included several categories of objects related to geologic settings of the Sunda Trench and Indonesia region: the location of trench and ridges, volcanoes, slabs, ophiolites, tectonic plate boundaries, focal mechanisms, showing the geological complexity of the region (Fig. 2). The sediment thickness map depicts the thickness of sediment layer with isolines plotted by each 1,000 m. The highest sediment thickness can be seen offshore the Kalimantan Island (blue, magenta to purple-colored areas Fig. 3) with values over 8,000 m, with the highest values (magenta color, >10,000 m) near the Brunei area, Brunei Bay (Fig. 3). Increased values of sediment thickness can be seen to the south-east off Kalimantan, Sulawesi, north-west Sumatra (green to cyan colors on Fig. 3), values from 3,000 to 7,000 m. That clearly points at the higher values of sediment in the Sumatra segment of the Sunda Trench comparing to the Java segment where dominating values are below 2,000 m (orange to red colors on Fig. 3).

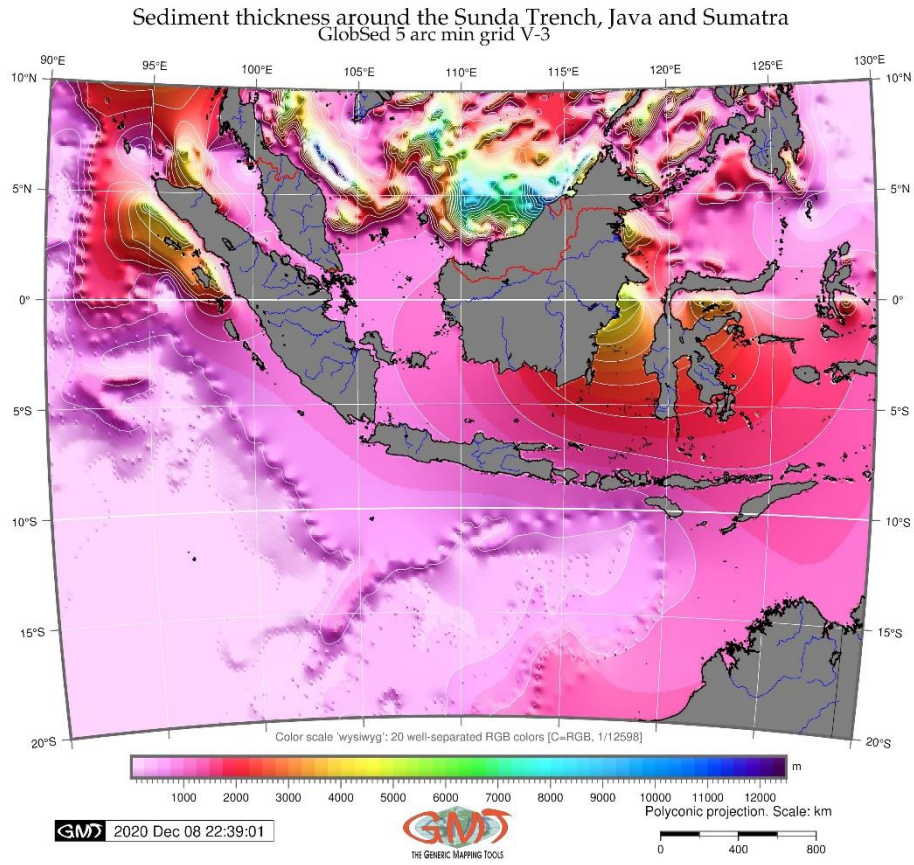

Fig. 3. Sediment thickness of the West Indonesia Basin (Source: Author)

The map of the geoid regional model (Fig. 4) clearly shows the asymmetric undulation over the study area: the higher categories of geoid undulation with values above 45 m (red colours on Fig. 4) are seen in the north-eastern part of the map in the north-eastern region of the Indonesia Archipelago, the Celebes Sea and the Philippine Sea basin continuing over the terrestrial area of Kalimantan and the Philippines. Comparing the topographic contour (Fig. 1) with geoid isolines (Fig. 4), one can see the correlation between the geophysical fields and topographic elevations. The area to the west of Kalimantan, Java, Sumatra, and the Thailand demonstrate gradual decrease in geoid values to -10 m (light orange to green colours on Fig. 4). The regions of Sumatra and northern Thailand show negative values decreasing further to the region of the Indian Ocean with values below 45 m (blue to dark blue colors, Fig. 4). As for the region of the Sunda Trench, it shows slightly negative values of the -30 to -10 m across the trench with a slight increase in its Java segment with 0 to -5 m (light aquamarine colour) comparing to Sumatra segment, -5 to -15 m (blueish to light cyan colour) (Fig. 4).

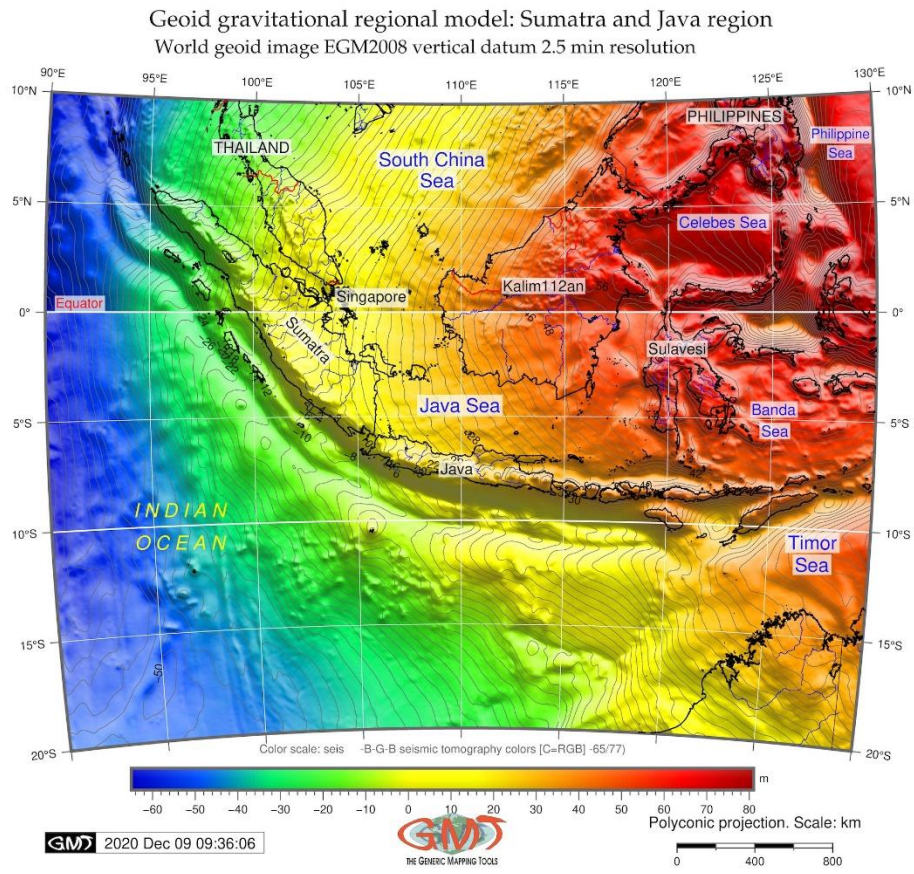

Fig. 4. Geoid model of the West Indonesia Basin (Source: Author)

The dominating free-air gravity values are notable for the range of -40 to 40 mGal (light aquamarine colour on Fig. 5). As for the regions of the Sunda Trench, it demonstrates lower values (-40 to -80 mgGal) correlating with the physiographic isolines of the bathymetric map (Fig. 1) which points at the dependences between the distribution of the elevations and the geophysical anomaly fields. The highest values of the marine free-air gravity with > 200 mGal (yellow to orange colours on Fig. 5) can be seen over the mountainous areas on Kalimantan and Indonesian archipelago, Sulawesi and central Thailand. The majority of the terrestrial area of Java and Sumatra indicate a correlation between gravity fields and topographic patterns of the mountains areas (Fig. 5).

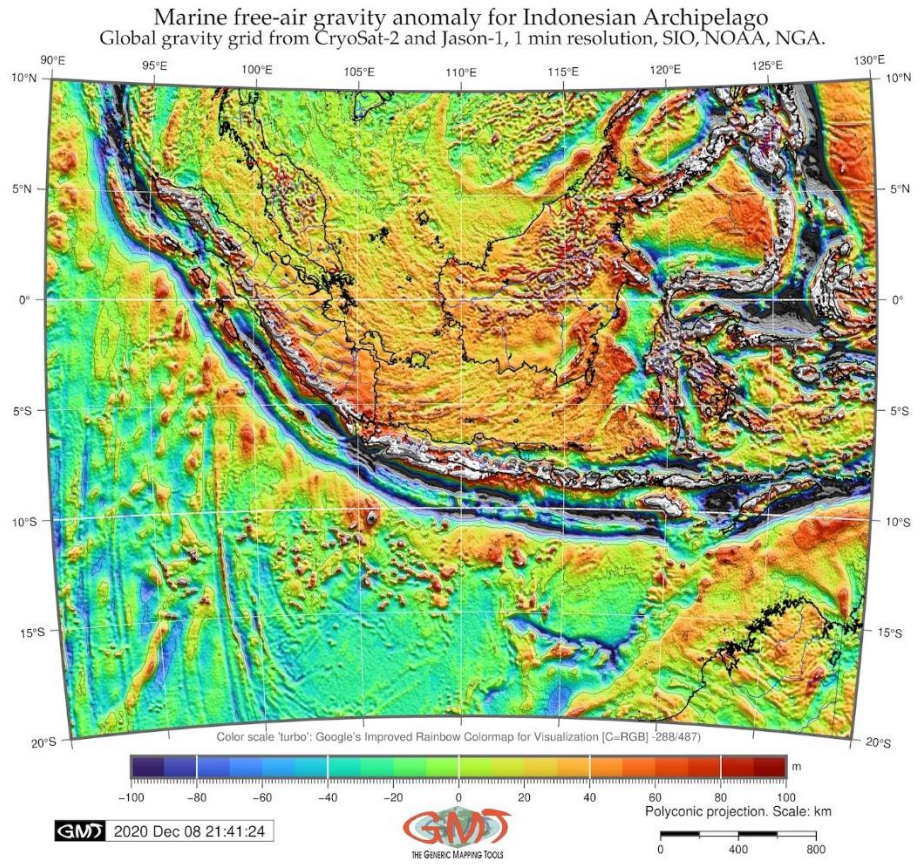

Fig. 5. Marine free-air gravity map of the West Indonesia Basin (Source: Author)

Comparison of the two segments of the Sunda Trench gives the following results: Sumatra, which is the northern (Fig. 6) and the Java, which is the southern (Fig. 7) shows that Java segment has a more symmetrical shape form while the Sumatra segment has a clear asymmetric one-sided shape. The Sumatra segment of Sunda Trench has a steepness of 57.86° on its eastern side (facing Sumatra Island) and a contrasting 14.58° on the western part facing the Indian Ocean (Fig. 6A). The digitized segment of Sumatra transect has coordinates 97.5°E 1.1°S to 101.0°E 5.5°S (Fig. 6B). The Java segment of Sunda Islands has a steepness of 64.34° on its northern side (facing Java Island) and 24.95° on the southern part facing the Indian Ocean (Fig. 7A).

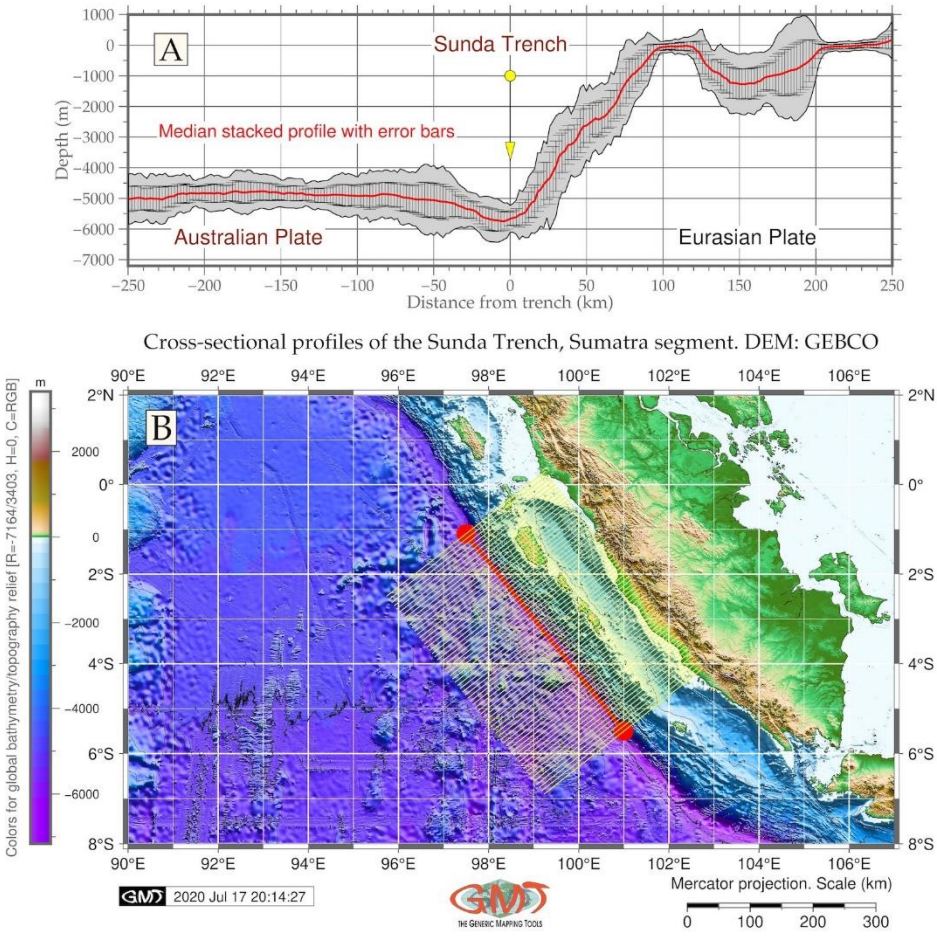

Fig. 6. Cross-section profiles of the Sunda Trench: Sumatra segment (Source: Author)

The digitized segment of Java transect has coordinates 108.8°E 10.10°S to 113.0°E 10.75°S, (Fig. 7B). In both cases the cross-track profiles are plotted as cross-track profiles 500 km long (250 km on each flank from the trench axis), sampled every 2 km, spaced 10 km between each perpendicular line which can be seen on Fig. 6B and 7B as a set of thin, parallel yellow-coloured lines. Despite the certain difference in a slope steepness of both flanks of the Java segment (Fig. 7), it has a more symmetric geometry form of the geomorphological profile comparing to the cross-section of the Sumatra segment (northern part of the Sunda Trench - Fig. 6).

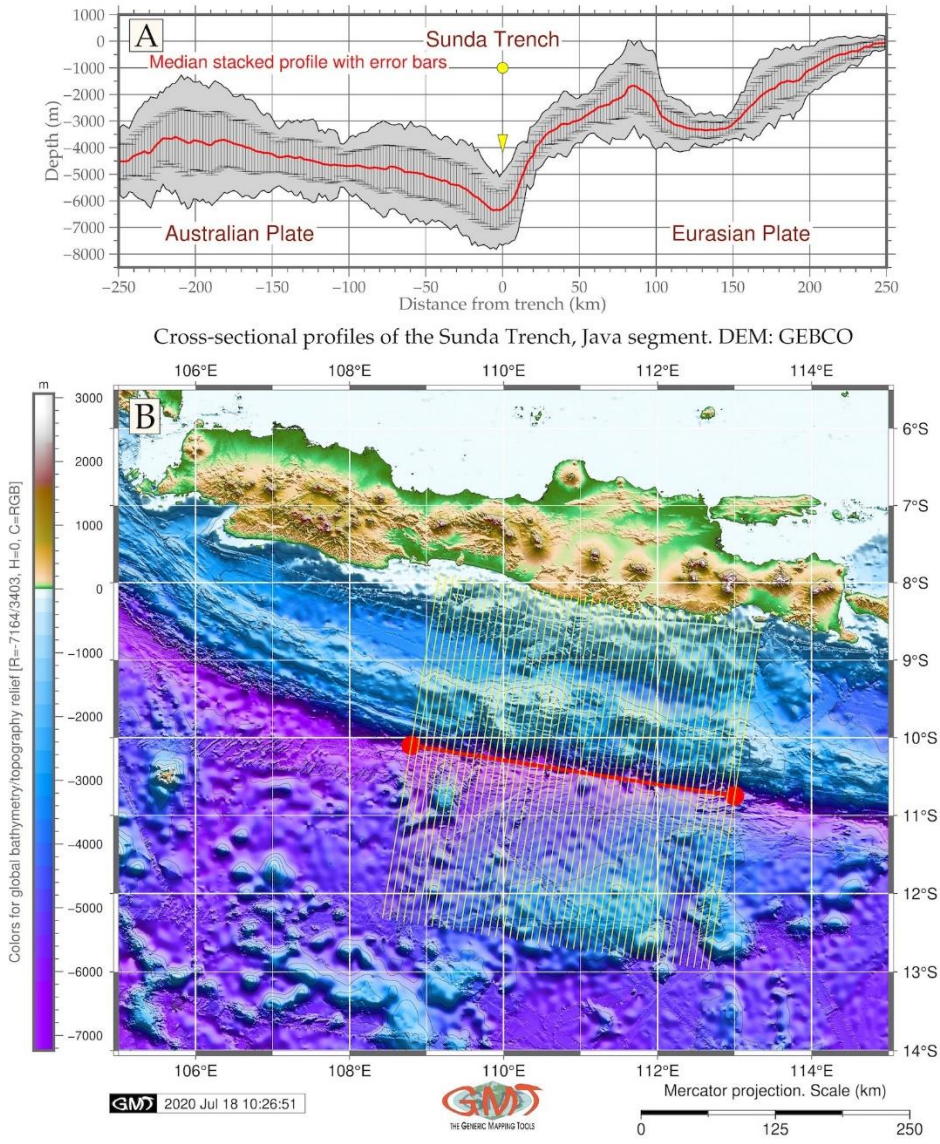

Fig. 7. Cross-section profiles of the Sunda Trench: Java segment (Source: Author)

The analysis of the statistical histograms (Fig. 8) shows variation in the frequency of the depths as data distributed along with the segments of the Sumatra and Java segments of the Sunda Trench. The Java Trench has a bell-shaped data distribution in contrast to the Sumatra segment which has a bimodal (two-peaked pattern) data distribution. The Java segment (Fig. 8, above) has a pool of data concentrating in the most repetitive depths in a bin with a range -2,500 to -5,200 m. The most repetitive data (above 700 samples) are recorded for the following bins: -3,500 to -3,750 m (816 samples), -3,250 to -3,500 m (811 samples), -4,750 to -5,000 m (791 samples), -2,750 to -3,000 m (743

samples) and -3,000 to -3,250 m (721 samples). It shows that in general, the majority of data are concentrated on the depths at -2,500 to -5,200 m.

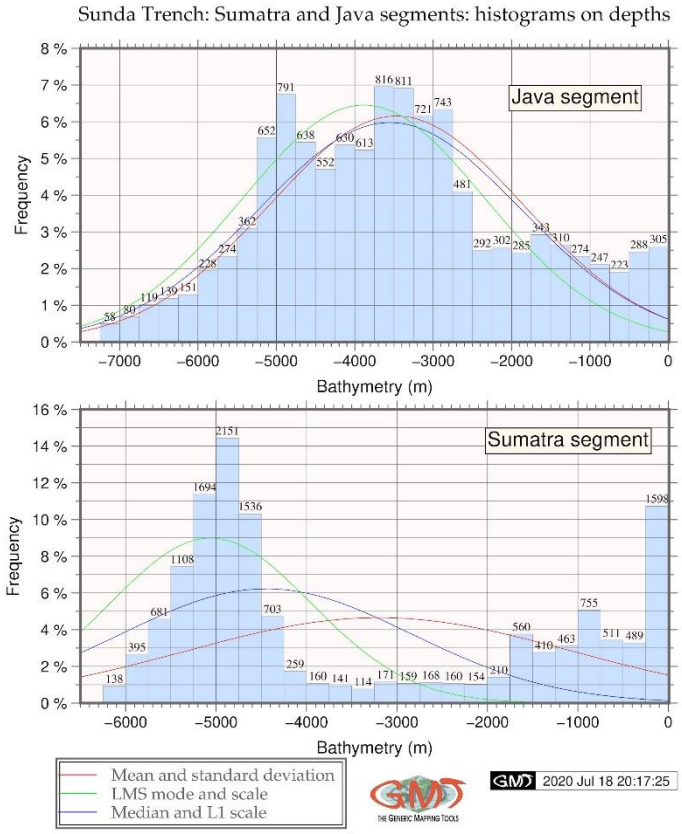

Fig. 8. Statistical histograms of the of the Sunda Trench (Source: Author)

The Sumatra segment of the Sunda Trench demonstrates a bimodal pattern of data distribution. Thus, in contrast with the Java transect, the Sumatra transect has the two peaks corresponding to the two intervals: 1) a classic bell-shaped peak at depths -4,500 m to -5,500 m with values above 600 samples in each bin; 2) a distinct shelf area with a peak from 0 to -1,750 m. The data at middle depths (between -1,750 to -4,500 m) have a frequency below 300 observation points. The most frequent bathymetric data for the Sumatra segment of the trench correspond to the bin of -4,750 m to -5,000 m (2,151 samples). Comparing to the Sumatra segment, the Java segment is in general deeper. For instance, if comparing the depths below -6,000 m, there are only 138 samples for the Sumatra segment while 547 samples for Java segment. Similarly, the middle -valued depths (those between -2,000 to -4,000 m) have less samples for the Sumatra segment than for the Java segment (compare both plots on Fig. 8). In the context of the regional topographic variations, the comparison of the histograms points at the difference in depth distribution for the Sumatra and Java segment of the Sunda Trench: a bimodal character of data distribution for a Sumatra segment Trench and a single-peaked data distribution

for a Java segment. Similarly, it shows the difference in depths: the southern Java segment shows to be deeper comparing to the Sumatra segment, and the geomorphology of the Sumatra segment has a clear asymmetric view comparing to the more V-shaped Java segment.

Discussion

Various methods of the geomorphological analysis have been discussed and described so far. To mention a few of them, these include geodetic measurements, terrain analysis, GIS-based applications (Gauger et al., 2007; Gao, 2009), modelling slopes and trends of the trenches (Lemenkova, 2019c, 2020f). By far the most effective use of cartographic approaches for geomorphological studies is for the cross-section profiling as demonstrating 2D transects of the study area and depicting various geomorphic landforms and slope steepness.

Geomorphological mapping of the submarine features and seafloor is developing rapidly along with the cartographic instruments and tools, and computer-based machine learning methods enabling effective data visualization, modelling, and mapping. However, besides technical advances, marine geomorphology largely depends on using key progress in general geosciences (geology, environment, landscape studies, tectonics) deriving new data and information from different frontier disciplines of Earth sciences. Such a multidisciplinary approach is highly advantageous for our better understanding of various geomorphological processes recorded at the seafloor. It also results in using different approaches to the geomorphological assessment and various mapping criteria.

Geomorphological mapping by GMT methods provides an effective means to visualize the seafloor, an important surface between the geological substrate and the ocean mass where a range of phenomena (biochemical, hydrological, oceanological) are controlled by the geomorphological shape of the submarine landforms and geological character of the seafloor. Although maps of seafloor geomorphology are important for a wide range of science branches (geology, oil and gas engineering, fisheries, and marine biological mapping), the cartographic techniques of the submarine geomorphological maps remain a challenge due to the remote location of the study object and the specifics of the GMT syntax. Besides, a submarine geomorphological mapping is strongly limited to the high-resolution data, that is a high-resolution GEBCO/SRTM topography grids.

The GMT techniques for mapping, cross-section digitizing and spatial modelling are an excellent alternative to classical GIS cartographic methods. In particular, scripting iterative methods enable to produce machine-plotted maps with higher precision compared to that achieved with hand-made methods of manual drawing in GIS. A drawback of console based cartographic scripting might be its high learning curve: a GMT does not have a standard GUI such as in ArcGIS (Klaučo et al., 2013a, 2013b) but only a console. However, in case of a processing large volumes of spatial multi-source data and a need of digitizing the cross-section segments for bathymetric and geomorphological mapping, scripting techniques of GMT represents an excellent solution to reduce the efforts during cartographic routine and to increase the precision of such unreachable areas as the deep-sea trenches.

Conclusion

The submarine geomorphology of the oceanic trenches is formed as a result of complex interactions between the processes of the tectonic plate subduction, geologic setting of the region and geodynamic. As a structural part of the ocean seafloor topography, the evolution of the oceanic trench reflects these changes mirrored in its actual shape which was discussed previously (Lemenkova, 2019i, 2019j). This suggests that submarine topography has mainly a dynamic character, being strongly influenced by both the previous geologic evolution and current external geophysical and geodynamic factors. The complexity of the natural phenomena and the connectivity and responses between various geological, geomorphic and climate factors are discussed previously (Widiyantoro et al., 2011).

Increased availability of high-resolution grids (GEBCO, EGM2008, SRTM) enables to better distinguish the genetic origin of seafloor landforms. Using datasets with a globe coverage allows better understood the context of the submarine geomorphological systems of the oceanic trenches in the context of the regional geophysical setting, geological development and tectonic history. Needless to say, that this progress has been facilitated by rapid development of the machine learning techniques, data science approaches and efforts in open data repositories by SIO, GEBCO, and last but not least, the progress in the computer hardware and memory which enables to process big datasets (e.g., original GEBCO grid with over 14 GB of size).

Geomorphological mapping strongly depends on the input data quality and resolution. Thus, bathymetric data can vary in terms of precision e.g., GEBCO 15 arc-second data acquired for visualizing seafloor versus regional-scale compilations from ETOPO1, ETOPO2 or ETOPO5 with 1, 2 and 5-minute resolution, respectively. The quality of initial bathymetric grids can facilitate delineation of geomorphological features in the processed output map layouts. In particular, it is true for the semi-automated techniques, as demonstrated by the GMT cross-sectional profiling. Higher resolution topographic raster grids increase the quality of the output geomorphological slope profiling. In contrary, poorer resolution cannot ensure the best results in geomorphological modelling. As mentioned before, this research is based on GEBCO 15 arc-second resolution topographic grid which ensured the quality and precision of the results.

Automated data processing approaches of GMT enables time-efficient precise and accurate cartographic visualization and geomorphological modelling using large data volumes, which replaces error-prone traditional, biased, manual interpretation of data. Besides, certain GMT modules ("pshistogram") provide statistical methods of data processing and descriptive statistical analysis. Automated methods of machine learning provided by GMT, as demonstrated in this paper, significantly reduce mapping subjectivity, labour time and mistakes. Human interpretation can be reduced to the interpretation of the layout outputs and writing the script. Human based geomorphological interpretation of the landforms can also be used for the description of natural complexity and analysis of the correlation with information of geological and tectonic evolution and geophysical settings of the trench formation.

Acknowledgments

This research was implemented in the framework of the project No. 0144-2019-0011, Schmidt Institute of Physics of the Earth, Russian Academy of Sciences.

References

Ashadi, A. L. & Kaka, S. I. (2019). Ground-Motion Relations for Subduction-Zone Earthquakes in Java Island, Indonesia. *Arabian Journal for Science and Engineering*, 44, 449–465. https://doi.org/10.1007/s13369-018-3563-x.

Audley-Charles, M. G., Ballantyne, P. D. & Hall, R. (1988). Mesozoic-Cenozoic rift-drift sequence of Asian fragments from Gondwanaland. *Tectonophysics*, 155, 317–330. https://doi.org/10.1016/0040-1951(88)90272-7.

Audley-Charles, M. G. (2004). Ocean trench blocked and obliterated by Banda forearc collision with Australian proximal continental slope. *Tectonophysics*, 389(1–2), 65–79. https://doi.org/10.1016/j.tecto.2004.07.048.

Becker, J. J., Sandwell, D. T., Smith, W. H. F., Braud, J., Binder, B., Depner, J., Fabre, D., Factor, J., Ingalls, S., Kim, S. H., Ladner, R., Marks, K., Nelson, S., Pharaoh, A., Trimmer, R., Von Rosenberg, J., Wallace, G. & Weatherall, P. (2009). Global bathymetry and elevation data at 30 arc seconds resolution: SRTM30_PLUS. *Marine Geodesy*, 32, 355–371.

Bird, P. (2003). An updated digital model of plate boundaries. *Geochemistry, Geophysics, Geosystems*, 4(3), 1027. https://doi.org/10.1029/2001GC000252.

Charlton, T. R. (2000). Tertiary evolution of the eastern Indonesia collision complex. *Journal of Asian Earth Sciences*, 18(5), 603–631. https://doi.org/10.1016/S1367-9120(99)00049-8.

Chlieh, M., Avouac, J. P., Sieh, K., Natawidjaja, D. H. & Galetzka, J. (2008). Heterogeneous coupling of the Sumatran megathrust constrained by geodetic and paleogeodetic measurements. *Journal of Geophysical Research*, 113, B05305. https://doi.org/10.1029/2007JB004981.

Das, S. (2004). Seismicity gaps and the shape of the seismic zone in the Banda Sea region from relocated hypocenters. *Journal of Geophysical Research*, 109, B12303. https://doi.org/10.1029/2004JB003192.

DeMets, C., Gordon, R. G. & Argus, D. F. (2010). Geologically current plate motions. *Geophysical Journal International*, 181, 1–80. https://doi.org/10.1111/j.1365-246X.2009.04491.x.

Dewi, R. S., Hartanto, P., Oktaviani, N., Pujawati, I., Nursugi, N. & Aditya, S. (2019). Satellite-derived bathymetry to improve bathymetric map of Indonesiaıo Proc. SPIE 11372, *Sixth International Symposium on LAPAN-IPB Satellite*, 113721N. https://doi.org/10.1117/12.2540779.

Ekström, G., Nettles, M. & Dziewoński, A. M. (2012). The global CMT project 2004–2010: Centroid-moment tensors for 13,017 earthquakes. *Physics of the Earth and Planetary Interiors*, 200, 1–9. https://doi.org/10.1016/j.pepi.2012.04.002.

Elburg, M. A., Foden, J. D., Van Bergen, M. J. & Zulkarnain, I. (2005). Australia and Indonesia in collision: Geochemical sources of magmatism. *Journal of Volcanology and Geothermal Research*, 140(1–3), 25–47. https://doi.org/10.1016/j.jvolgeores.2004.07.014.

Ely, K. S. & Sandiford, M. (2010). Seismic response to slab rupture and variation in lithospheric structure beneath the Savu Sea, Indonesia. *Tectonophysics*, 483(1–2), 112–124. https://doi.org/10.1016/j.tecto.2009.08.027.

Gao, J. (2009). Bathymetric mapping by means of remote sensing: methods, accuracy and limitations. *Progress in Physical Geography: Earth and Environment*, 33(1), 103-116. https://doi.org/10.1177/0309133309105657.

Gasparon, M., Hilton, D. R. & Varne, R. (1994). Crustal contamination processes traced by helium isotopes: Examples from the Sunda arc, Indonesia. *Earth and Planetary Science Letters*, 126(15–22). https://doi.org/10.1016/0012-821X(94)90239-9.

Gauger, S., Kuhn, G., Gohl, K., Feigl, T., Lemenkova, P. & Hillenbrand, C. (2007). Swath-bathymetric mapping. *Reports on Polar and Marine Research*, 557, 38–45. https://doi.org/10.6084/m9.figshare.7439231.

GEBCO Compilation Group (2020). GEBCO 2020 Grid. Retrieved from https://doi.org/10.5285/a29c5465-b138-234d-e053-6c86abc040b9.

GDAL/OGR contributors (2020). GDAL/OGR Geospatial Data Abstraction Software Library. Open-Source Geospatial Foundation. https://gdal.org [Online Accessed: 8 December 2020].

Gohl, K., Eagles, G., Udintsev, G., Larter, R. D., Uenzelmann-Neben, G., Schenke, H.-W., Lemenkova, P., Grobys, J., Parsiegla, N., Schlueter, P., Deen, T., Kuhn, G. & Hillenbrand, C.-D. (2006a). Tectonic and sedimentary processes of the West Antarctic margin of the Amundsen Sea embayment and PineIsland Bay. *2nd SCAR Open Science Meeting*, 12-14 Jul, Hobart, Australia. https://doi.org/10.6084/m9.figshare.7435484.

Gohl, K., Uenzelmann-Neben, G., Eagles, G., Fahl, A., Feigl, T., Grobys, J., Just, J., Leinweber, V., Lensch, N., Mayr, C., Parsiegla, N., Rackebrandt, N., Schlüter, P., Suckro, S., Zimmermann, K., Gauger, S., Bohlmann, H., Netzeband, G. & Lemenkova, P. (2006b). Crustal and Sedimentary Structures and Geodynamic Evolution of the West Antarctic Continental Margin and Pine Island Bay. *Expeditionsprogramm* Nr.75 ANT XXIII/4 ANT XXIII/5, 11–12. https://doi.org/10.13140/RG.2.2.16473.36961.

Gunawan, E., Ghozalba, F., Syauqi, Widiastomo, Y., Meilano, I., Hanifa, N. R., Daryono & Hidayati, S. (2017). Field Investigation of the November to December 2015 Earthquake Swarm in West Halmahera, Indonesia. *Geotechnical and Geological Engineering*, 35(1) 425–432 https://doi.org/10.1007/s10706-016-0117-4.

Harris, R. (2011). The nature of the Banda Arc–continent collision in the Timor region. In *Arc-continent collision*, 163–211. Berlin, Heidelberg: Springer. https://doi.org/10.1007/978-3-540-88558-0_7.

Harris, P. T., Macmillan-Lawler, M., Rupp, J. & Baker, E.K. (2014). Geomorphology of the oceans. Marine Geology, 352, 4–24. https://doi.org/10.1016/j.margeo.2014.01.011.

Harris, C. W., Miller, M. S., Supendi, P. & Widiyantoro, S. (2020). Subducted Lithospheric Boundary Tomographically Imaged Beneath Arc-Continent Collision in Eastern Indonesia. *Journal of Geophysical Research*. Solid Earth, 125(8), e2019JB018854. https://doi.org/10.1029/2019JB018854.

Haryanto, I., Ilmi, N. N., Hutabarat, J., Gumelar, B., Adhiperdana, Fauzielly, L., Andriana, Y., Sendjaja & Sunardi, E. (2020). Tectonic and geological structures of Gunung Kromong, West Java, Indonesia. *International Journal of GEOMATE*, 19(74), 185–193. https://doi.org/10.21660/2020.74.05449.

Hinschberger, F., Malod, J. A., Dyment, J., Honthaas, C., Rehault, J. P. & Burhanuddin, S. (2001). Magnetic lineations constraints for the back-arc opening of the Late Neogene South Banda Basin (eastern Indonesia). *Tectonophysics*, 333(1–2), 47–59. https://doi.org/10.1016/S0040-1951(00)00266-3.

Honthaas, C., Réhault, J.P., Maury, R. C., Bellon, H., Hémond, C., Malod, J.A., Cornée, J.J., Villeneuve, M., Cotten, J., Burhanuddin, S., Guillou, H. & Arnaud, N. (1998). A Neogene back-arc origin for the Banda Sea basins: Geochemical and geochronological constraints from the Banda ridges (East Indonesia). *Tectonophysics*, 298, 297–317. https://doi.org/10.1016/S0040-1951(98)00190-5.

Hughes, B. D., Baxter, K., Clark, R. A., & Snyder, D. B. (1996). Detailed processing of seismic reflection data from the frontal part of the Timor trough accretionary wedge, eastern Indonesia. Geological Society, London, *Special Publications*, 106(1), 75–83. https://doi.org/10.1144/GSL.SP.1996.106.01.07.

IHO-IOC. (2012). GEBCO Gazetteer of Undersea Feature Names.

Kawamura, K., Kuranaga, M. & Mochizuki, K. (2017). Early Diagenesis of Deep-Sea Sediments on Incoming Plates: Examples from the Izu-Bonin Trench and the Sunda Trench. *GSA Annual*

Meeting in Seattle, Washington, USA, Paper No. 115-7. https://doi.org/10.1130/abs/2017AM-296938.

Kawamura, K., Kuranaga, M., Mochizuki, K. & Kanamatsu, T. (2020). The role of pre-subduction sediment diagenesis in a shallow tsunami-generated slip, Sunda Trench, south of Sumatra. Geological Society, London, *Special Publications*, 501, https://doi.org/10.1144/SP501-2019-44.

Klaučo, M., Gregorová, B., Stankov, U., Marković, V. & Lemenkova, P. (2013a). Determination of ecological significance based on geostatistical assessment: a case study from the Slovak Natura 2000 protected area. *Central European Journal of Geosciences*, 5(1), 28–42. https://doi.org/10.2478/s13533-012-0120-0.

Klaučo, M., Gregorová, B., Stankov, U., Marković, V. & Lemenkova, P. (2013b). Interpretation of Landscape Values, Typology and Quality Using Methods of Spatial Metrics for Ecological Planning. *54th International Conference Environmental & Climate Technologies*. Riga, Latvia. https://doi.org/10.13140/RG.2.2.23026.96963.

Klaučo, M., Gregorová, B., Stankov, U., Marković, V. & Lemenkova, P. (2014). Landscape metrics as indicator for ecological significance: assessment of Sitno Natura 2000 sites, Slovakia. *Ecology and Environmental Protection*, 85–90. https://doi.org/10.6084/m9.figshare.7434200.

Klaučo, M., Gregorová, B., Stankov, U., Marković, V. & Lemenkova, P. (2017). Land planning as a support for sustainable development based on tourism: A case study of Slovak Rural Region. *Environmental Engineering and Management Journal*, 2(16), 449–458. https://doi.org/10.30638/eemj.2017.045.

Kreemer, C., Holt, W. E., Goes, S. & Govers, R. (2000). Active deformation in eastern Indonesia and the Philippines from GPS and seismicity data. *Journal of Geophysical Research*, 105(B1), 663–680. https://doi.org/10.1029/1999JB900356.

Kuhn, G., Hass, C., Kober, M., Petitat, M., Feigl, T., Hillenbrand, C. D., Kruger, S., Forwick, M., Gauger, S. and Lemenkova, P. (2006): The response of quaternary climatic cycles in the South-East Pacific: development of the opal belt and dynamics behavior of the West Antarctic ice sheet. In: Gohl, K. (ed). *Expeditionsprogramm* Nr. 75 ANT XXIII/4, AWI. https://doi.org/10.13140/RG.2.2.11468.87687.

Lemenkova, P. (2011). Seagrass Mapping and Monitoring Along the Coasts of Crete, Greece. M.Sc. Thesis. Netherlands: University of Twente, 158 https://doi.org/10.13140/RG.2.2.16945.22881

Lemenkova, P., Promper, C., & Glade, T. (2012). Economic Assessment of Landslide Risk for the Waidhofen a.d. Ybbs Region, Alpine Foreland, Lower Austria. In: Eberhardt E, Froese C, Turner AK, Leroueil S. (eds.) Protecting Society through Improved Understanding. *11th International Symposium on Landslides & the 2nd North American Symposium on Landslides & Engineered Slopes (NASL)*, June 2–8, 2012. Banff, Canada, 279–285. https://doi.org/10.6084/m9.figshare.7434230.

Lemenkova, P. (2018). R scripting libraries for comparative analysis of the correlation methods to identify factors affecting Mariana Trench formation. *Journal of Marine Technology and Environment*, 2, 35–42. https://doi.org/10.6084/m9.figshare.7434167.

Lemenkova, P. (2019e). Plotting Ternary Diagrams by R Library ggtern for Geological Modelling. *Eastern Anatolian Journal of Science*, 5(2), 16–25. https://doi.org/10.6084/m9.figshare.11369955.

Lemenkova, P. (2019d). Geomorphological modelling and mapping of the Peru-Chile Trench by GMT. *Polish Cartographical Review*, 51(4), 181–194. https://doi.org/10.2478/pcr-2019-0015.

Lemenkova, P. (2019c). An Empirical Study of R Applications for Data Analysis in Marine Geology. *Marine Science and Technology Bulletin*, 8(1), 1–9. https://doi.org/10.33714/masteb.486678.

Lemenkova, P. (2019b). Automatic Data Processing for Visualizing Yap and Palau Trenches by Generic Mapping Tools. *Cartographic Letters*, 27(2), 72–89. https://doi.org/10.6084/m9.figshare.11544048.

Lemenkova, P. (2019a). Geospatial Analysis by Python and R: Geomorphology of the Philippine Trench, Pacific Ocean. *Electronic Letters on Science and Engineering*, 15(3), 81–94. https://doi.org/10.6084/m9.figshare.11449362.

Lemenkova, P. (2020a). Geomorphology of the Puerto Rico Trench and Cayman Trough in the Context of the Geological Evolution of the Caribbean Sea. *Annales Universitatis Mariae Curie-Sklodowska, sectio B – Geographia, Geologia, Mineralogia et Petrographia*, 75, 115-141. https://doi.org/10.17951/b.2020.75.115-141.

Lemenkova, P. (2020b). Visualization of the geophysical settings in the Philippine Sea margins by means of GMT and ISC data. *Central European Journal of Geography and Sustainable Development*, 2(1), 5–15. https://doi.org/10.47246/CEJGSD.2020.2.1.1.

Lemenkova, P. (2020c). GMT-based geological mapping and assessment of the bathymetric variations of the Kuril-Kamchatka Trench, Pacific Ocean. *Natural and Engineering Sciences*, 5(1), 1–17. https://doi.org/10.28978/nesciences.691708.

Lemenkova, P. (2020d). Using GMT for 2D and 3D Modeling of the Ryukyu Trench Topography, Pacific Ocean. *Miscellanea Geographica*, 25(3), 1-13. https://doi.org/10.2478/mgrsd-2020-0038.

Lemenkova, P. (2020e). GEBCO Gridded Bathymetric Datasets for Mapping Japan Trench Geomorphology by Means of GMT Scripting Toolset. *Geodesy and Cartography*, 46 (3), 98–112. https://doi.org/10.3846/gac.2020.11524.

Lemenkova, P. (2020f). Integration of geospatial data for mapping variation of sediment thickness in the North Sea. *Scientific Annals of the Danube Delta Institute*, 25, 129–138. https://doi.org/10.7427/DDI.25.14.

Lemenkova, P. (2020g). The geomorphology of the Makran Trench in the context of the geological and geophysical settings of the Arabian Sea. *Geology, Geophysics and Environment*, 46(3), 205–222. https://doi.org/10.7494/geol.2020.46.3.205.

Lemenkova, P. (2020h). Insights on the Indian Ocean tectonics and geophysics supported by GMT. *Risks and Catastrophes Journal*, 27(2), 67–83. https://doi.org/10.24193/RCJ2020_12.

Lemenkova, P. (2020i). Seafloor Mapping of the Atlantic Ocean by GMT: Visualizing Mid-Atlantic Ridge Spreading, Sediment Distribution and Tectonic Development. *Acta Geobalcanica*, 6(3), 145-157. https://doi.org/10.18509/AGB.2020.16.

Maemunah, I., Suparka, E., Puspito, N. T. & Hidayati, S. (2015). Sedimentary deposits study of the 2006 Java tsunami, in Pangandaran, West Java (preliminary result). *AIP Conference Proceedings*, 1658, 050005. https://doi.org/10.1063/1.4915044.

McCloskey, J., Lange, D., Tilmann, F., Nalbant, S. S., Bell, A. F., Hilman, D., Natawidjaja & Rietbrock, A. (2010). The September 2009 Padang earthquake. *Nature Geoscience*, 3, 70–71. https://doi.org/10.1038/ngeo753.

Megawati, K. & Pan, T.-C. (2010). Ground-motion attenuation relationship for the Sumatran megathrust earthquakes. *Earthquake Engineering and Structural Dynamics*, 39(8), 827–845. https://doi.org/10.1002/eqe.967.

Nalbant, S. S., Steacy, S., Sieh, K., Natawidjaja, D. & McCloskey, J. (2005). Earthquake risk on the Sunda trench. *Nature*, 435, 756–757. https://doi.org/10.1038/nature435756a.

Nalbant, S., McCloskey, J., Steacy, S., NicBhloscaidh, M. & Murphy, S. (2013), Interseismic coupling, stress evolution, and earthquake slip on the Sunda megathrust. *Geophysical Research Letters*, 40, 4204– 4208, https://doi.org/10.1002/grl.50776.

Natawidjaja, D. H. & Triyoso, W. (2007). The Sumatran fault zone –from source to hazard. J*ournal of Earthquake and Tsunami*, 1, 21-47.https://doi.org/10.1142/S1793431107000031.

Nishimura, S. & Suparka, S. (1990). Tectonics of East Indonesia. *Tectonophysics*, 181, 257-266. https://doi.org/10.1016/0040-1951(90)90019-5.

Nurwihastuti, D. W., Sartohadi, J., Mardiatno, D., Nehren, U. & Restu. (2014). Understanding of Earthquake Damage Pattern through Geomorphological Approach: A Case Study of 2006 Earthquake in Bantul, Yogyakarta, Indonesia. *World Journal of Engineering and Technology*, 02(3B), 61– 70. https://doi.org/10.4236/wjet.2014.23B010.

Patria, A. & Aulia, A. N. (2020). Structural and Earthquake Evaluations Along Java Subduction Zone, Indonesia. *RISET Geologi dan Pertambangan*, 30(1), (65-79). https://doi.org/10.14203/risetgeotam2020.v30.1074.

Pavlis, N. K., Holmes, S. A., Kenyon, S. C. & Factor, J. K. (2012). The development and evaluation of the Earth Gravitational Model 2008 (EGM2008). *Journal of Geophysical Research*, 117, B04406, https://doi.org/10.1029/2011JB008916.

Pickering, K. T., Pouderoux, H., McNeill, L.C., Backman, J., Chemale, F., Kutterolf, S., Milliken, K. L., Mukoyoshi, H., Henstock, T. J., Stevens, D. E., Parnell, C. & Dugan, B. (2020). Sedimentology, stratigraphy and architecture of the Nicobar Fan (Bengal–Nicobar Fan System), Indian Ocean: Results from International Ocean Discovery Program Expedition 362. *Sedimentology*, 67: 2248-2281. https://doi.org/10.1111/sed.12701.

Plank, T. & Langmuir, C. (1994). A. view from the Sunda arc. *Nature*, 367, 224–225 https://doi.org/10.1038/367224b0.

Poetra, R. P., Adji, T. N., Santosa, L. W. & Khakhim, N. (2020). Hydrogeochemical Conditions in Groundwater Systems with Various Geomorphological Units in Kulonprogo Regency, Java Island, Indonesia. *Aquatic Geochemistry*, 26, 421–454. https://doi.org/10.1007/s10498-020-09384-w.

Saito, T. & Kubota, T. (2020). Tsunami Modeling for the Deep Sea and Inside Focal Areas. *Annual Review of Earth and Planetary Sciences*, 48:1, 121–145.

Salman, R., Lindsey, E. O., Feng, L., Bradley, K., Wei, S., Wang, T., Daryono, M. R. & Hill, E. M. (2020). Structural controls on rupture extent of recent Sumatran Fault Zone earthquakes, Indonesia. *Journal of Geophysical Research: Solid Earth*, 125, e2019JB018101. https://doi.org/10.1029/2019JB018101.

Sandwell, D. T., Müller, R. D., Smith, W. H. F., Garcia, E. & Francis, R. (2014). New global marine gravity model from CryoSat-2 and Jason-1 reveals buried tectonic structure. *Science*, 346(6205), 65–67. https://doi.org/10.1126/science.1258213.

Schenke, H. W. & Lemenkova, P. (2008). Zur Frage der Meeresboden-Kartographie: Die Nutzung von AutoTrace Digitizer für die Vektorisierung der Bathymetrischen Daten in der Petschora-See. *Hydrographische Nachrichten* 81, 16–21. https://doi.org/10.6084/m9.figshare.7435538

Sieh, K. & Natawidjaja, D. (2000), Neotectonics of the Sumatran fault, Indonesia, *J. Geophys. Res.,* 105(B12), 28295–28326, https://doi.org/10.1029/2000JB900120.

Straume, E. O., Gaina, C., Medvedev, S., Hochmuth, K., Gohl, K., Whittaker, J. M., Abdul Fattah, R., Doornenbal, J. C. & Hopper, J. R. (2019). GlobSed: Updated total sediment thickness in the world's oceans. *Geochemistry, Geophysics, Geosystems*, 20(4), 1756–1772. https://doi.org/10.1029/2018GC008115.

Suetova, I. A., Ushakova, L. A. & Lemenkova, P. (2005). Geoinformation mapping of the Barents and Pechora Seas. *Geography and Natural Resources*, 4, 138–142. https://doi.org/10.6084/m9.figshare.7435535.

Tabei, T., Kimata, F., Ito, T., Gunawan, E., Tsutsumi, H., Ohta, Y., Yamashina, T., Soeda, Y., Ismail, N., Nurdin, I., Sugiyanto, D. & Meilano, I. (2015). Geodetic and Geomorphic Evaluations of Earthquake Generation Potential of the Northern Sumatran Fault, Indonesia. In: Hashimoto M. (eds). *International Symposium on Geodesy for Earthquake and Natural Hazards (GENAH)*. International Association of Geodesy Symposia, 145. Springer, Cham. https://doi.org/10.1007/1345_2015_200.

Titisari, A. D., Phillips, D., Prayatna & Setyaraharja, E. P. (2017). 40Ar/39Ar Geochronology of Volcanic and Intrusive Rocks in the Papandayan Metallic Prospect Area, West Java, Indonesia. *Resource Geology*, 67: 53– 71. https://doi.org/10.1111/rge.12118.

Tozer, B., Sandwell, D.T., Smith, W.H.F., Olson, C., Beale, J.R., & Wessel, P. (2019). Global bathymetry and topography at 15 arc sec: SRTM15+. *Earth and Space Science*, 6(10), 1847–1864 https://doi.org/10.1029/2019EA000658.

Verstappen, H. T. (2014). Indonesian Landforms and Plate Tectonics. *Indonesian Journal on Geoscience*, 5(3). https://doi.org/10.17014/ijog.5.3.197-207.

Weatherall, P., Marks, K. M., Jakobsson, M., Schmitt, T., Tani, S., Arndt, J. E., Rovere, M., Chayes, D., Ferrini, V. & Wigley, R. (2015). A new digital bathymetric model of the world's oceans. *Earth and Space Science*, 2(8), 331–345. https://doi.org/10.1002/2015EA000107.

Wessel, P. & Smith, W. H. F. (1996). A Global Self-consistent, Hierarchical, High-resolution Shoreline Database. *Journal of Geophysical Research*, 101, 8741–8743. https://doi.org/10.1029/96JB00104.

Wessel, P., Smith, W. H. F., Scharroo, R., Luis, J. F. & Wobbe, F. (2013). Generic mapping tools: Improved version released. *Eos Transactions of the American Geophysical Union*, 94(45), 409–410. https://doi.org/10.1002/2013EO450001.

Widiyantoro, S., Gunawan, E., Muhari, A., Rawlinson, N., Mori, J., Hanifa, N. R., Susilo, S., Supendi, P., Shiddiqi, H. A., Nugraha, A. D. & Putra, H. E. (2020). Implications for megathrust earthquakes and tsunamis from seismic gaps south of Java Indonesia. *Scientific Reports*, 10, 15274. https://doi.org/10.1038/s41598-020-72142-z.

Winarto, J. B., Sukiyah, E., Haryanto, A. D. & Haryanto, I. (2019). Sub Surface Active Fault Identification on Quaternary and Tertiary Rocks using Geoelectric Method in Cilaki Drainage Basin, Southern Part of West Java, Indonesia. *International Journal on Advanced Science*, Engineering and Information Technology, 9(5), 1563–1569. http://dx.doi.org/10.18517/ijaseit.9.5.8111.

Полина Леменкова*

* *Институт за физику Земље О. Шмита, Руска академија наука, Департман за природне непогоде, хазарде и сеизмичност Земље, Лабораторија за регионалну геофизику и природне непогоде, Москва, Руска Федерација*

ГЕОМОРФОЛОШКЕ И ГЕОФИЗИЧКЕ КАРАКТЕРИСТИКЕ ЈАВАНСКОГ И СУМАТРАНСКОГ СЕГМЕНТА ВЕЛИКОГ СУНДСКОГ РОВА АНАЛИЗИРАНЕ И ВИЗУЕЛИЗОВАНЕ КОРИШЋЕЊЕМ GMT

Резиме: У раду су детаљно анализиране геоморфолошке карактеристике Сундског рова, који се пружа дуж острва Суматра и Јава у оквиру индонежанског архипелага, у источном делу Индијског океана. Познато је да је геоморфологија океанских ровова настала као резултат субдукције тектонских плоча током сложене геолошке еволуције. Упркос покушајима да се детаљно проучи његова геодинамика, природа и структура рова још увек нису довољно јасни. Конкретно, геоморфолошке карактеристике рова, формиране кроз сложене интеракције геофизичких, геолошких и тектонских фактора, у фокусу су многих истраживања. Сврха овог рада је да истражи разлике у геоморфолошким карактеристикама два различита сегмента Сундског рова (јужни део дуж острва Јава и северни део дуж острва Суматра) како би се олакшало боље разумевање структуре морског дна у североисточном делу Индијског океана. Методолошки приступ овог рада заснован је на употреби GMT, односно универзалних картографских инструмената, који су примењени у циљу конструисања графичких прилога. У овом квалитативном и квантитативном истраживању израђено је осам карата и обављен је преглед бројне литературе о истраживаном подручју.

Јужни, јавански сегмент рова простире се дуж линије са следећим координатама (почетна и крајња тачка): 108,8°E 10,10°S - 113,0°E 10,75°S. Северни, суматрански сегмент лоциран је дуж линије са следећим координатама (почетна и крајња тачка) 97,5°E 1,1°S - 101,0°E 5,5°S. Подаци укључују растерску координатну мрежу високе резолуције о топографији, геологији, геодезији и геофизици: GEBCO, EGM2008EGM-2008, GlobSed. Представљено је и визуализовано неколико тематских карата са циљем демонстрирања просторне варијације у дистрибуцији геофизичких поља на проучаваном подручју. Карте посебно илуструју геолошке процесе који су се одвијали у источном делу Индијског океана у различитим фазама његове еволуције, а које су утицале на изглед подморске геоморфологије рова. Попречни профили су дигитализовани помоћу приступа машинског учења којег нуди GMT. Упоредна анализа оба сегмента извршена је визуелизацијом података у виду хистограма. Резултати истраживања показују да је геоморфологија рова зависна од локалних геолошких, геофизичких и тектонских карактеристика. Конкретно, јавански сегмент има дистрибуцију дубина у "облику звона", за разлику од суматранског са бимодалном дистрибуцијом. У сегменту Јаве најчешће је распрострањен појас дубина између -2.500 и -5.200 m. Сегмент Суматре има два јасно видљива врха: 1) врх у облику звона (-4.500 m до -5.500 m); 2) подручје шелфа (0 до -1.750 m). У поређењу са сегментом Суматре (северни), сегмент Јаве (јужни) је дубљи. На пример, за дубине преко -6.000 m постоји само 138 узорака за сегмент

Суматре, док постоји 547 узорака за сегмент Јаве. Даље, јавански сегмент има симетричан геометријски облик, док је сегмент Суматре углавном асиметричан. Сегмент Суматре има нагиб од 57,86° на источној страни (страна окренута према острву Суматра) и 14,58° на западној страни. Сегмент Јаве има нагиб од 64,34° на северној страни (страна окренута према острву Јава) и 24,95° у јужном делу (према Индијском океану).

Значај картографске визуелизације је добро познат, јер тачно представљање података помаже да се изврши корелација и укаже на разлике у дистрибуцији геолошких и географских објеката, процеса и појава. Најчешће, традиционални GIS софтвери преовлађују у картографским истраживањима. Овај рад указује на ефикасну функционалност софтвера GMT за визуализацију геофизичких и геолошких података и за проучавање геоморфолошких карактеристика. Нејасност и неразумевање геолошких и геодинамичких процеса често проистиче из недостатка картографске визуализације која покрива одређено истраживачко подручје у правилној пројекцији и палети боја. Да би се повећала ефикасност у анализи података, представљене карте конструисане су у три различите пројекције: поликонусној, меркаторовој и азимутној пројекцији Ламберта, док су попречни профили урађени са декартовим *xy* координатама. Значај овог рада састоји се у мултидисциплинарном приступу који комбинује савремена картографска представљања података и геолошку анализу индонежанског региона. Резултати ове студије показују да су коришћење картографских метода за обраду геоинформација драгоцено средство за даља геофизичка и геоморфолошка моделовања и помоћ у бољем разумевању морског дна, јединствене скривене структуре Земљине површине.